



# Detection of early stage Alzheimer's disease in gradient-based MR images using deep learning methods

## Derin öğrenme yöntemleri kullanılarak gradyan tabanlı MR görüntülerinde erken safha Alzheimer hastalığının tespiti

Mehmet Emre Sertkaya<sup>1,\*</sup> , Meryem Durmuş<sup>2</sup> , Burhan Ergen<sup>3</sup> 

<sup>1,2</sup> Samsun University, Center for Distance Education, 55000, Samsun, Türkiye

<sup>3</sup> Fırat University, Computer Engineering Department, 23119, Elazığ, Türkiye

### Abstract

Alzheimer's Disease (AD), a form of dementia prevalent in older age, is a neurodegenerative condition impacting brain nerve cells. Early-stage AD symptoms are often subtle, complicating timely diagnosis. Early detection allows for intervention, slowing disease progression and facilitating appropriate treatments. Deep learning methods, particularly gradient-based images, prove promising for early Alzheimer's detection in Magnetic Resonance (MR) imaging. Gradient-based images, highlighting details in low-intensity images and enhancing contrast, play a vital role in determining structures' location, shape, and size, notably in techniques like Magnetic Resonance Imaging (MRI). This study aims to boost model performance in early AD detection by applying the Gradient filter before training deep learning models on diverse-angle and constant-density brain MRI images. The dataset comprises three categories representing early-stage AD, including images of Mild cognitive impairment and healthy individuals. Original and gradient-filtered image subsets were inputted into deep learning models. Results indicate superior performance of gradient-based images, with the Densenet201 deep learning model achieving the highest accuracy at 98.63%.

**Keywords:** Alzheimer's disease, Deep learning techniques, Gradient filter, Magnetic resonance images, Mild cognitive impairment.

### 1 Introduction

Alzheimer's Disease (AD) is a progressive disease that causes the loss of brain cells, the exact cause of which is still unknown. AD results in permanent damage to memory cells and leads to dementia. AD, the most common form of dementia, causes cognitive and behavioral problems. It is an irreversible degenerative disease that leads to physical and mental decline over time [1]. The amount of protein accumulation in the nerve cells in the brain increases over

### Öz

Alzheimer Hastalığı (AD), genellikle yaşlılık döneminde görülen bir demans türüdür. AD, beynin sinir hücrelerine yavaşça zarar veren bir nörodejeneratif hastalıktır. Erken evre AD belirtileri genellikle hafif ve tipik olmayan olduğundan teşhisi zorlaştırır. Ancak erken teşhis, hastalığın ilerlemesini yavaşlatma ve uygun tedavi seçenekleri sunma açısından müdahaleyi mümkün kılar. Derin öğrenme yöntemleri, özellikle Manyetik Rezonans (MR) görüntülerinde ince detayları tespit etmek için kullanılabilir. Bu yöntemler, özellikle Manyetik Rezonans Görüntüleme (MRG) gibi görüntüleme tekniklerinde, çeşitli yapıların konumunu, şeklini ve boyutunu belirlemede gradyan tabanlı görüntülerin önemli bir rol oynadığı düşünülmektedir. Bu çalışma, farklı açılardaki ve sabit yoğunluktaki beyin MR görüntülerini eğitmek için Derin Öğrenme modellerine önce Gradient filtresi uygulayarak Alzheimer hastalığının erken tespiti konusundaki modellerin performansını artırmayı amaçlamaktadır. Erken aşama AD'yi temsil eden üç farklı kategoriden oluşan görüntü veri seti, hafif bilişsel bozukluğa sahip bireylerin ve sağlıklı bireylerin görüntülerini içermektedir. Orijinal ve gradyan filtrelenmiş görüntü alt kümeleri, derin öğrenme modellerine giriş olarak kullanılmıştır. Çalışma sonuçları, gradyan tabanlı görüntülerin derin öğrenme modellerinde orijinal görüntülerden daha iyi bir performans sergilediğini göstermektedir. Densenet201 derin öğrenme modeli %98,63'lük en yüksek doğruluk oranını elde etmiştir.

**Anahtar Kelimeler:** Alzheimer hastalığı, Derin öğrenme Teknikleri, Gradyan filtre, Manyetik rezonans görüntüleri, Hafif bilişsel bozukluk.

time. Due to the protein buildup in nerve cells, the connections between nerve cells in the brain gradually break down. This condition damages nerve cells and leads to cell death over time [2].

Mild cognitive impairment (MCI), which negatively affects social activities, is an early stage that precedes AD. MCI is also known as a transitional stage between cognitive decline or memory loss associated with aging and early dementia [3]. Early diagnosis of AD is critical to take

\* Sorumlu yazar / Corresponding author, e-posta / e-mail: emre.sertkaya@samsun.edu.tr (M. E. Sertkaya)

Geliş / Recieved: 14.11.2023 Kabul / Accepted: 15.03.2024 Yayınlanma / Published: xx.xx.20xx

doi: 10.28948/ngumuh.1390830

preventative measures that can slow the progression of the disease. Technological advancements in the field have had a positive impact on the healthcare industry [4]. These advancements have reduced the workload for patients and their families. Aging is a natural process of human life. The improvement in healthcare and social well-being has positively affected both the lifespan and quality of life. Dementia, which has a high incidence of aging, has become an important burden in society due to its negative impact on the social lives of both patients and their relatives [5].

The course of the disease can be significantly influenced by treatment initiated at the MCI stage. Therefore, early diagnosis of AD is of great importance [6, 7]. However, despite recent advances in AD research, the complexity of brain structure and functions makes early diagnosis of this disease challenging [6]. Magnetic Resonance Imaging (MRI) enables investigation of the brain's anatomical structure by analyzing various neurological diseases and pathological regions [8]. In recent years, significant progress has been observed in the evaluation of brain injuries and the investigation of brain anatomy using MRI. Disorders such as AD and brain-related multiple sclerosis can be diagnosed using MRI [9]. Convolutional Neural Networks (CNN) have made significant progress in image recognition for AD diagnosis using MRI and Positron Emission Tomography (PET) [8].

F. Ramzan et al. [10] worked on the ADNI dataset containing MR images of 138 individuals. They used the ResNet-18 architecture as a classification method and first trained the ADNI dataset using residual learning, pre-training, and transfer learning. The OTS network they created achieved an accuracy of 97.92% for 6 disease stages.

Helaly H. et al. [11] aim to design an end-to-end framework for early detection and stage classification of Alzheimer's disease. The four-stage Alzheimer's spectrum is multiclassified using convolutional neural networks (CNN). Furthermore, binary medical image classifications were performed between both stages. Simple CNN architectures and pre-trained models were used to process 2D and 3D brain scans using two methods. A web application is proposed to provide remote Alzheimer's checkup when regular visits to hospitals are difficult due to COVID-19. Experimental results showed that the CNN architectures used in the first method achieved high accuracy with appropriate simple structures, e.g., 93.61% and 95.17% for 2D and 3D multi-classification AD stages, respectively. Moreover, the VGG19 pre-trained model achieved 97% accuracy with fine-tuning.

A. Mehmood et al. [12] studied the open-access OASIS data series with 382 MR images. They used data augmentation techniques to expand the imbalanced dataset and increase the data volume. To classify dementia stages, they developed the SCNN model inspired by the VGG-16 architecture. With their proposed approach, they classified the stages of dementia with an accuracy rate of 99.05%.

Mujahid M. et al. [13] built a unified model that learns complex and nuanced patterns from data by combining the predictions of multiple models. The input and output of both models, EfficientNet-B2 and VGG-16, were combined to

create a unified model and then added to other layers to obtain a more robust model. In order to diagnose the disease at an early stage with the highest accuracy, the experiments were conducted on a dataset collected from two publicly available Kaggles. The experimental results show that the proposed method achieves 97.35% accuracy and 99.64% AUC for multiclass datasets and 97.09% accuracy and 99.59% AUC for binary class datasets. They observed that the proposed method is highly effective and offers superior performance on both datasets compared to previous methods.

A. Farooq et al. [14] used the ADNI dataset to diagnose AD and its stages using MR images. To perform multi-class classification of AD, mild cognitive impairment (MCI), late mild cognitive impairment (LMCI), and healthy individuals, they applied a CNN-based 4-classifier. The ADNI dataset, consisting of a total of 38,024 images, including 9506 images for each class, was tested using GoogLeNet, ResNet-18, and ResNet-152 models, achieving an accuracy of 98.8%.

R. Ibrahim et al. [15] presents a new hybrid model that combines the Particle Swarm Optimization (PSO) algorithm with CNNs. Their method used the PSO algorithm to determine the optimal configuration of CNN hyperparameters. Then, these optimized parameters are applied to CNN architectures for classification. As a result, our hybrid model exhibits improved prediction accuracy for brain diseases while reducing loss of function. They applied their proposed method on 3 different data sets. The first two data sets were used for Alzheimer's disease: Alzheimer's Disease Neuroimaging Initiative (ADNI) and an international dataset from Kaggle. The third dataset focused on brain tumors. Experimental evaluation showed that their proposed model achieved accuracy rates of 98.50%, 98.83% and 97.12%, respectively.

Sarraf, S., and Tofighi, G. [5] tried to predict AD stages for different age groups by applying the LeNet-5 architecture on MR images in the ADNI dataset. They achieved an accuracy of 96.85% on test data.

Balaji P. et al. [16] proposes a hybrid Deep Learning Approach for early diagnosis of Alzheimer's disease. A method for early diagnosis of Alzheimer's disease using multiple imaging and Long Short Term Memory algorithm combines magnetic resonance imaging (MRI), positron emission tomography (PET) and standard neuropsychological test scores. The proposed methodology updates learning weights and uses Adam optimization to improve accuracy. The system has an unmatched 98.5% accuracy in classifying cognitively normal controls from ADHDS. These results demonstrate that deep neural networks can be trained to automatically discover imaging markers indicative of AD and accurately identify the disease.

Basaia, S. et al. [17] achieved a 99% accuracy in differentiating AD and MCI patients from healthy individuals and accurately predicting the conversion of MCI to AD within 36 months using a LeNet model. The study used 3D T1-weighted images from a total of 1409 individuals (294 AD, 763 MCI, and 352 healthy controls). At the end of the 36-month period, 253 MCI cases were clinically observed to have converted to AD. The AD and

healthy control groups were classified with a 99% accuracy using the ADNI dataset and 98% accuracy using both the ADNI and an external dataset.

Liu, S. et al. [18] propose a multi-class deep learning architecture consisting of MCI, the prodromal stage of AD, content autoencoders and softmax output layer that enable early diagnosis. They worked with the ADNI dataset, which contained a total of 311 individuals with 65 AD, 169 MCI, and 77 healthy controls, and their proposed method achieved a higher accuracy of 87.76% compared to SVM.

The significance of this study lies in providing an approach for the early diagnosis of Alzheimer's Disease by utilizing brain MR images obtained from different perspectives. The objective of the article is to enhance the early diagnosis performance of Alzheimer's Disease by comparing various model architectures using the Gradient Filter. The Gradient Filter plays a crucial role in detecting subtle details in Magnetic Resonance (MR) images. Specifically, when applied to brain MR images obtained from different angles and constant intensity, the Gradient Filter ensures a more precise processing of the images. Consequently, the obtained results contribute to determining the best model architecture that demonstrates a more effective performance in the early diagnosis of Alzheimer's Disease. The summary of this study by section is as follows: this section provides information on the dataset to be used in Section 2. Section 3 contains information on deep learning models, filtering methods, and the proposed approach. Section 4 presents Experimental Analysis and Discussion results. The final section consists of the Conclusion.

## 2 Dataset

The dataset used in this study consists of open-access MR images of 3 classes of patients, Alzheimer Disease (AD), Cognitive Normal (CN), and Mild Cognitive Impairment (MCI), which are published on Kaggle [19]. The image distributions of the classes are shown in Table 1. The image distributions of the classes in the dataset have a homogeneous distribution, and sample images belonging to the classes are shown in Figure 1.

**Table 1.** Dataset classes and image counts

| Classes               | Number of MR Images |
|-----------------------|---------------------|
| Alzheimer's Disease   | 459                 |
| Cognitive Normal      | 489                 |
| Mild Cognitive Normal | 507                 |

As shown in Figure 1, the MR images of each class in this dataset are T2-weighted images taken from different angles of the brain. Although these MR images are taken from different angles, they have different contrast intensities. The images in the dataset were split into 70% for training and 30% for testing the models.

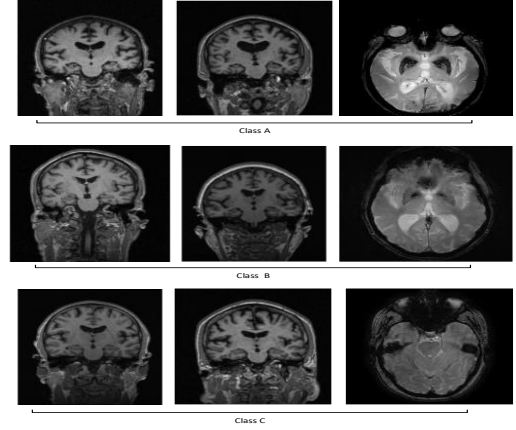


**Figure 1.** Example images of dataset classes a)AD; b)CN; c)MCI

## 3 Methodology

### 3.1 Deep learning methods

Deep learning is a machine learning paradigm for solving complex tasks and is built on the multi-layered and complex structures of artificial neural networks. This approach is used to learn and represent patterns in large data sets. Basically, a deep learning model contains multiple successive layers, starting from an input layer. Each layer learns to represent the features in the previous layer at a higher level. This deep structure increases the neural network's capacity to learn complex and abstract features [20]. Activation functions determine the output of each neural cell and make these outputs non-linear. This non-linearity allows the deep learning model to more effectively model complex relationships between input data. Backpropagation algorithms are used to adjust the weights during the training of the model. This process allows the model to learn patterns in data sets and then make successful predictions on new data [21]. Deep learning stands out for its potential to achieve effective results, especially on large-scale data sets and high-dimensional data tasks. Today, it has been successfully applied in many fields such as image recognition, natural language processing, game strategies and automated driving. Therefore, deep learning has become an important tool for solving complex problems and achieving significant success in real-world applications [22]. Figure 2 below shows the layer structure of deep learning.

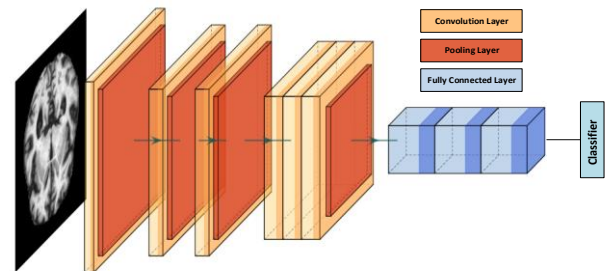


**Figure 2.** Deep learning model structure

Deep learning models consist of multiple different layers. The differences in these layers and their depth create the deep

learning models. The input layer converts images to pixel value matrices and forwards them to the next layer as either single-channel or multi-channel depending on the type of image.

The convolution layer uses a series of filter matrices to extract local patterns and features from the input data. These filters contain weights, each designed to emphasize certain features. Mathematically, the convolution process involves shifting a filter matrix over the input data and performing an inner product operation at each position. Each filter learns the weights to detect a particular feature or pattern, and thus different filters increase the learning capacity of the model [23]. These filters are usually used to learn low-level features, e.g. simple patterns such as edges, corners. Then, successive convolution layers combine these low-level features to learn more complex and high-level features. For example, the filters in the first layer may be able to detect edges, while the filters in the second layer may be geared towards learning simple geometric patterns that are combinations of these edges [24]. As a result, convolution layers allow features to be extracted in a hierarchical way over images or other types of data. This allows the model to learn appropriate features for more complex and abstract tasks.

The activation layer is an important component of the convolution layer that adds nonlinearity by handling the outputs. Expressed mathematically, this layer subjects each element in the input data to an activation function. The activation function is used to increase the learning capacity of the network and enable the model to better represent complex, nonlinear relationships. The Rectified Linear Unit (ReLU) is a commonly used activation function. Mathematically, the ReLU function is a linear function in which the negative part of the input equals zero and the positive part is retained [25].

This function is particularly favored for speeding up the learning process of the network and reducing the computational cost. Moreover, the nonlinearity provided by ReLU contributes to the network learning more complex and hierarchical features. The activation layer, with such an activation function applied to the outputs of the convolution layer, allows the model to represent more complex and learnable features on top of the input data. This increases the generalization ability of the network and makes the learning process more effective [25].

The pooling layer is a layer used to sharpen the most important features and reduce the size of the matrix it receives. This layer reduces the number of parameters in the fully connected layer, reducing the complexity of the model and eliminating problems such as overfitting. The average pooling method can effectively reduce the influence of image noise, but it destroys the structural information of the image. On the other hand, maximum pooling can reduce the convolutional error and effectively preserve the structural information of the image, which is why it is commonly used. The fully connected layer is a type of layer in the deep learning model that is used especially in classification tasks. This layer flattens features from previous layers and is designed to assign a vector containing these features to one or more classes. Finally, the output layer, which is the

classifier layer, categorizes the feature permutation received from the fully connected layer using classification methods [26-28].

Multiple deep learning methods were used in this study, including VGG16, VGG19, Resnet50, Resnet101, Densenet201, and Mobilenet models. The VGG16 model used in this study consists of 13 convolutional layers and 3 pooling layers, and exhibits successful results even with small image datasets [29].

VGG19, developed by Visual Geometry Group (VGG) like VGG16, has a structure consisting of convolutional layers arranged in groups of two and four [30].

The Densenet201 deep learning model differs from other models in that activation functions are combined instead of being added to the next layer. Therefore, the activation layers from previous layers are kept in all layer types in addition to the original data. Since there are short connections between the input and output layers in this architecture, this model is said to be denser and more efficient [31-33].

The Mobilenet model was developed in 2017 for mobile applications. This architecture uses Depthwise Separable Convolutions technique for feature extraction instead of the classic Convolutional layer, which performs feature extraction with 8 or 9 times less parameters than normal convolution technique [31, 34].

The other two models used in the study, Resnet50 and Resnet101 models, consist of 50 and 101 layers respectively. Although increasing the number of layers is thought to extract more distinctive features, it has been observed that the performance of multi-layer models decreases compared to models with fewer layers due to gradient loss. The Resnet models solve this problem by using additional shortcut connections that prevent this loss without adding extra parameters or computational complexity, called forward propagation [35, 36].

### 3.2 Gradient filter method

The Morphological Gradient is a filtering technique that consists of a series of steps to emphasize shapes in image data. This technique uses two methods called erosion and dilation. Dilation enlarges the new output image by adding pixels to the image boundary and reduces the space between pixels. The erosion function removes pixels at the edges of the image and removes noise from the image. The gradient method uses these two techniques and corresponds to the difference between them [37-39].

The purpose of the gradient method is to sharpen the edges of objects for each input image. In the process of sharpening object edges, a threshold value is set and multiplied by this value. In this process, the multiplier value is considered as the bit depth value. This process is applied at each iteration stage to sharpen the object edges [37-39]. Figure 3 shows examples of images obtained after applying the Gradient filter to the original images. Figure 4. shows the proposed approach.

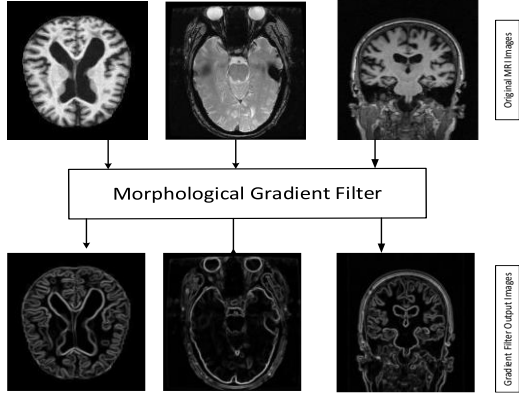


Figure 3. Gradient filter outputs

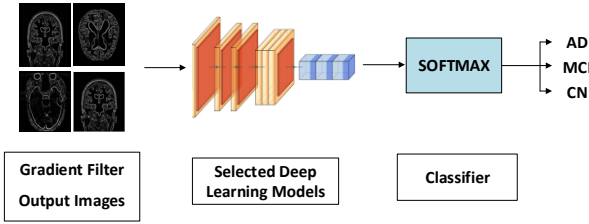


Figure 4. Proposed approach

#### 4 Experiment analysis and discussion

The software implementation environment of this study consisting of 2 experiments was realized using MATLAB (2022a). The specifications of the computer used in the compilation of MATLAB software are; 12 GB graphics card, 32 GB memory, AMD Ryzen 7 3800X 8- Core processor with 3.9 GHz speed and Windows 10 64-bit operating system. In the analysis, class-based metric values were obtained using the complexity matrix. The complexity matrix metrics used in this study are Sensitivity (Se), Precision (Sp), Specificity (Pre), F-score (F-scr), and Accuracy (Acc). The equations for the metric measures are shown below in Equations 1-5 [40].

$$Se = \frac{TP}{TP + FN} \quad (1)$$

$$Sp = \frac{TN}{TN + FP} \quad (2)$$

$$Pre = \frac{TP}{TP + FP} \quad (3)$$

$$F - scr = \frac{2xTP}{2xTP + FP + FN} \quad (4)$$

$$Acc = \frac{TP + TN}{TP + TN + FP + FN} \quad (5)$$

The grayscale images of the dataset were preprocessed with the desired input size and then divided into a 70-30 ratio for training and testing. During the training process, which involved 2250 iterations and utilized a batch size of 16 examples for each step, the Adam optimization algorithm

with a learning rate of 0.0001 was chosen for optimization. The models were trained using these deep parameters, and throughout the training process, the input image size remained configured as 256x256x1.

In the first experiment, deep learning methods were employed to classify the proposed approach using the original Alzheimer's dataset images. Subsequently, in the second experiment, prior to presenting the dataset images to CNN models, disease features were enhanced by applying a Gradient filter. The resulting images, sharpened with the Gradient filter, were fed into CNN models for classification. This process was repeated with the newly obtained images. To ensure an accurate comparison, the same CNN models and parameters were used in both experiments.

The aim of these 2 experiments is to investigate the contribution of preprocessing to the performance of the model before feeding the images to the CNN models. In the first experiment, the original data set and CNN models were used to determine the performance of the models. Figure 5 shows the Training and Validation performance graphs of 6 CNN models. When the graphs are analyzed, a steady linear increase is observed in the training and validation graphs. In training, the Densenet201 and Vgg16 models showed the best performance, while in the validation graph, the performance fluctuations in iterations tried to find local and global maximum. Densenet201 and Resnet-101 models showed the best performance in validation.

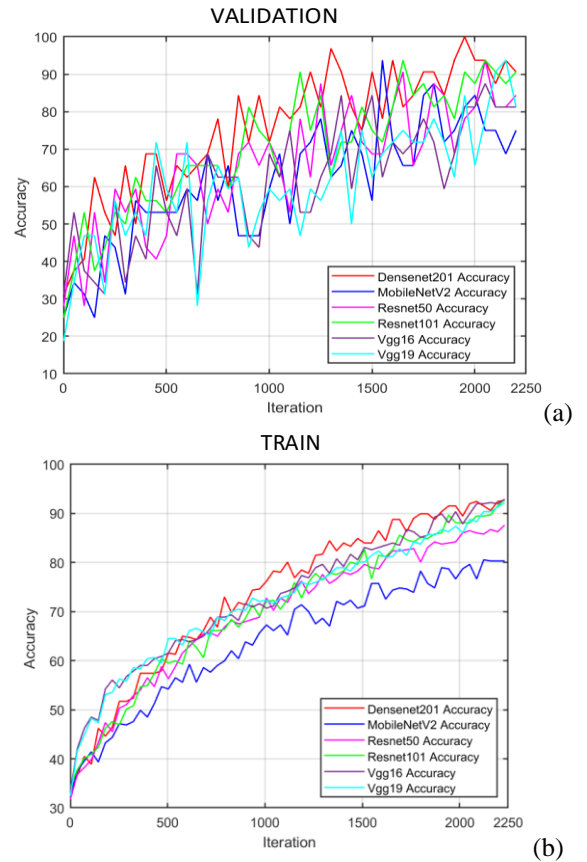


Figure 5. a)Verification and b)training performance graphs of deep learning models given original images

Confusion matrices obtained from CNN models are shown in Figure 6. The analysis results obtained based on the confusion matrices are shown in Table 2. When Table 2 is analyzed, the Densenet201 model showed the best performance among CNN models with an overall accuracy rate of 97.94%. In second place in terms of performance, the Resnet101 CNN model exhibits an overall accuracy rate of 94.05%. The lowest performance is the MobileNetV2 CNN model with 86.96% accuracy rate.

These performance values are not only the overall performance but also have the same performance ranking when analyzed on a class basis. When analyzed on a class basis, it is seen in Table 2 that the MCI class decreases the overall performance and exhibits lower performance compared to other classes. It is thought that the reason for this is that the parameters determining this stage are not very clear or that it occurs in different regions of the brain in each patient, since MCI is considered to be the preliminary or early stage of AD transition stage.

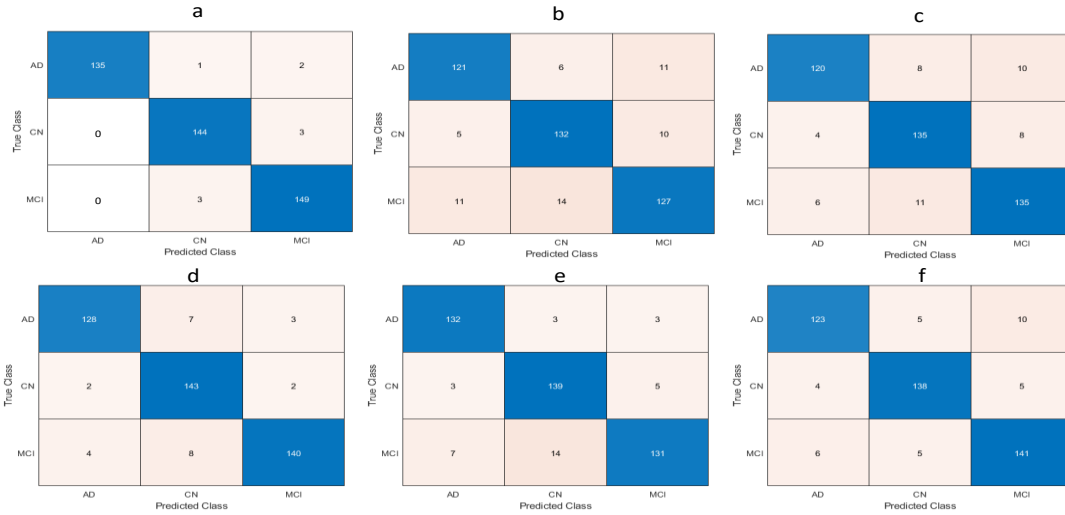


Figure 5. Confusion matrix of deep learning models given original images matrisi a)Densenet201, b)MobileNetV2, c)Resnet50, d)Resnet101, e)Vgg16, f)Vgg19

Table 2. First experimental group analysis results based on complexity matrices

| MODEL              | Class | Se.(%) | Sp.(%) | Pre.(%) | F-Scr. | Acc.(%) | Overall Achievement (%) |
|--------------------|-------|--------|--------|---------|--------|---------|-------------------------|
| <b>Densenet201</b> | AD    | 97.83  | 100.00 | 100.00  | 0.989  | 99.31   | 97.94                   |
|                    | CN    | 97.96  | 99.48  | 97.30   | 0.976  | 98.40   |                         |
|                    | MCI   | 99.53  | 98.24  | 99.22   | 0.973  | 98.17   |                         |
| <b>Resnet101</b>   | AD    | 92.75  | 97.92  | 95.52   | 0.941  | 96.34   | 94.05                   |
|                    | CN    | 97.28  | 94.70  | 90.51   | 0.937  | 95.65   |                         |
|                    | MCI   | 92.11  | 98.19  | 96.55   | 0.942  | 96.11   |                         |
| <b>Vgg16</b>       | AD    | 95.65  | 96.43  | 92.96   | 0.942  | 96.34   | 91.99                   |
|                    | CN    | 94.56  | 93.93  | 89.10   | 0.917  | 94.28   |                         |
|                    | MCI   | 86.18  | 97.13  | 94.24   | 0.900  | 93.36   |                         |
| <b>Resnet50</b>    | AD    | 86.96  | 96.43  | 92.31   | 0.895  | 93.59   | 89.24                   |
|                    | CN    | 91.84  | 93.07  | 87.66   | 0.897  | 92.91   |                         |
|                    | MCI   | 88.82  | 93.41  | 88.24   | 0.885  | 91.99   |                         |
| <b>Vgg19</b>       | AD    | 89.13  | 96.54  | 92.48   | 0.907  | 94.28   | 91.99                   |
|                    | CN    | 93.88  | 96.35  | 93.24   | 0.935  | 95.65   |                         |
|                    | MCI   | 92.76  | 94.57  | 90.38   | 0.915  | 94.05   |                         |
| <b>MobileNetV2</b> | AD    | 87.68  | 94.18  | 88.32   | 0.88   | 92.54   | 86.96                   |
|                    | CN    | 89.80  | 92.54  | 86.84   | 0.882  | 91.99   |                         |
|                    | MCI   | 83.55  | 92.34  | 85.81   | 0.846  | 89.47   |                         |

In the second experimental study phase, the images of the dataset were preprocessed using a gradient filter before being fed to the model. The new images obtained were given to the CNN models in the first experimental study and classification was performed. Training and validation performance graphs of these 6 CNN models are shown in Figure 7. Confusion matrices obtained from CNN models are shown in Figure 8. When the validation and training graphs are compared with the training and validation graphs in Figure 5, it is seen that the performance of the models using Gradient filtered images is more stable and the performance of the Densenet201, MobileNetV2 and ResNet models increases. Correspondingly, the validation performance is better for all models.

The analysis results obtained depending on the confusion matrices are shown in Table 3. When Table 3 is analyzed, the best performance was 98.63% for the Densenet201 CNN Model as in the first experiment. The VGG19 CNN model showed the lowest performance with 80.09%. When Table 3 is compared with Table 2 in the first experiment, it is observed that the use of gradient filtered images is not a performance enhancing factor in all CNN models. While the overall accuracy of Densenet201, Resnet101 and VGG16 models increased, the overall accuracy of Resnet50, VGG19 and MobilenetV2 models decreased. The reason for this is thought to be due to other parameters of the models rather than the layer structure.

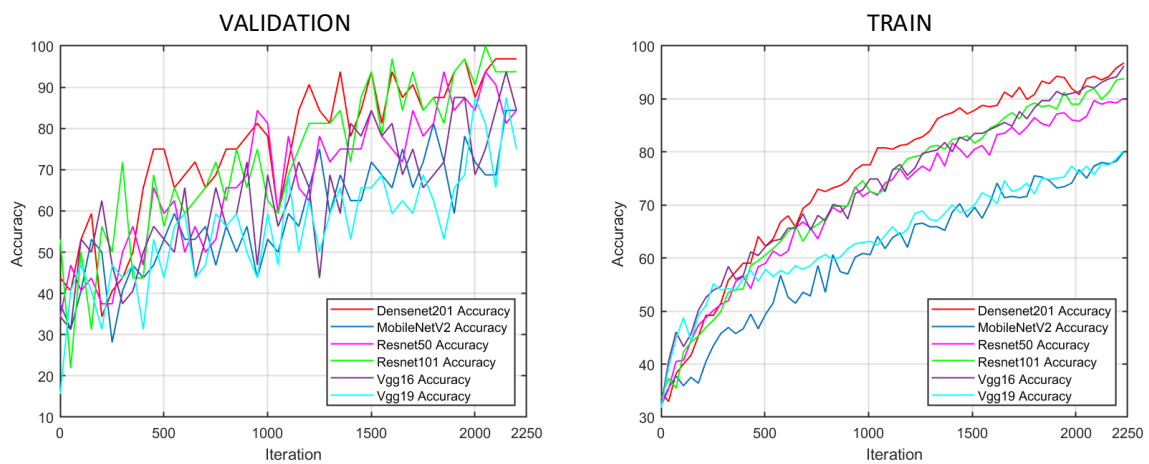


Figure 6. Validation and training performance graphs for deep learning models of output images from gradient filter

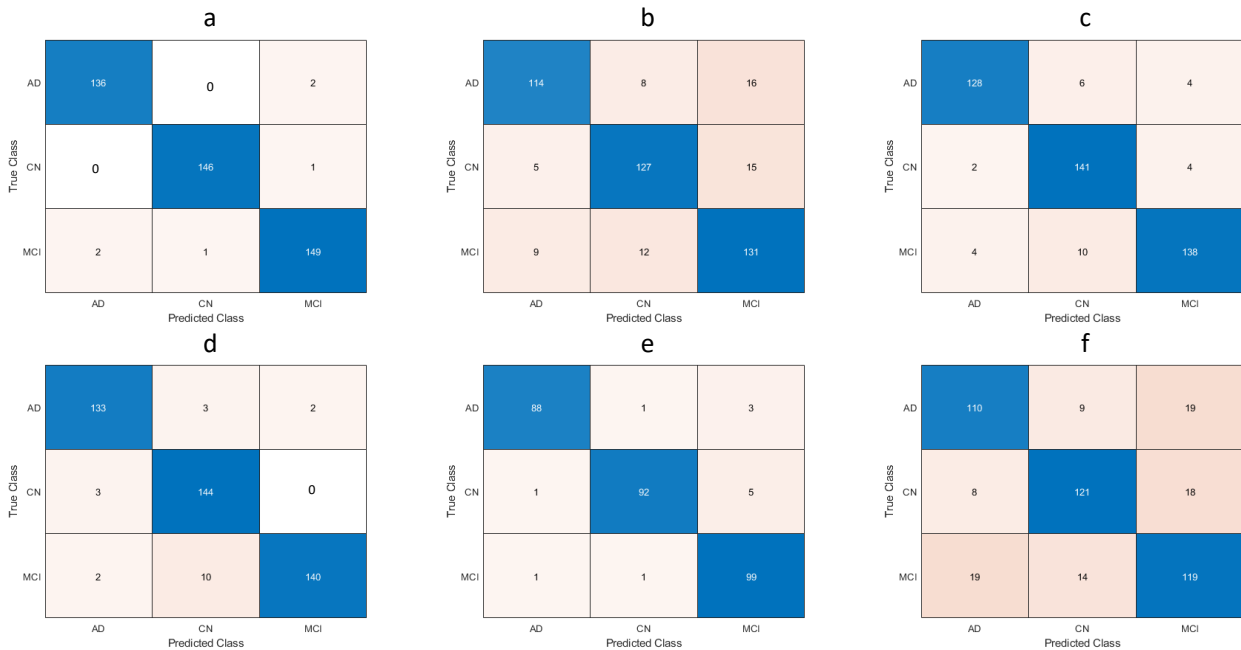


Figure 7. Confusion matrix for deep learning models of output images obtained from gradient filter: a)Densenet201, b)Mobilenetv2, c)Resnet50, d)Resnet101, e)Vgg16, f)Vgg19

**Table 3.** 2. Analysis results based on the complexity matrices of the experiment

| MODEL              | Class | Se.(%) | Sp.(%) | Pre.(%) | F-Scr. | Acc.(%) | Overall Achievement (%) |
|--------------------|-------|--------|--------|---------|--------|---------|-------------------------|
| <b>DenseNet201</b> | AD    | 98.55  | 99.33  | 98.55   | 0.985  | 99.08   | <b>98.63</b>            |
|                    | CN    | 99.32  | 99.65  | 99.32   | 0.993  | 99.54   |                         |
|                    | MCI   | 98.03  | 98.95  | 98.03   | 0.980  | 98.63   |                         |
| <b>Resnet101</b>   | AD    | 96.38  | 98.27  | 96.38   | 0.963  | 97.71   | 95.42                   |
|                    | CN    | 97.96  | 95.45  | 91.72   | 0.947  | 96.34   |                         |
|                    | MCI   | 92.11  | 99.28  | 98.59   | 0.952  | 96.8    |                         |
| <b>Vgg16</b>       | AD    | 95.65  | 98.96  | 97.78   | 0.967  | 97.94   | 95.88                   |
|                    | CN    | 93.88  | 98.94  | 97.87   | 0.958  | 97.25   |                         |
|                    | MCI   | 98.02  | 95.74  | 92.52   | 0.951  | 96.56   |                         |
| <b>Resnet50</b>    | AD    | 92.75  | 97.89  | 95.52   | 0.941  | 96.34   | 93.14                   |
|                    | CN    | 95.92  | 94.33  | 89.81   | 0.927  | 94.97   |                         |
|                    | MCI   | 90.79  | 97.11  | 94.52   | 0.926  | 94.97   |                         |
| <b>Vgg19</b>       | AD    | 79.71  | 89.89  | 80.29   | 0.8    | 87.41   | 80.09                   |
|                    | CN    | 82.31  | 90.87  | 84.03   | 0.831  | 88.79   |                         |
|                    | MCI   | 78.29  | 86.19  | 76.28   | 0.772  | 83.98   |                         |
| <b>MobileNetV2</b> | AD    | 82.61  | 94.85  | 89.06   | 0.857  | 91.3    | 85.13                   |
|                    | CN    | 86.39  | 92.45  | 86.39   | 0.863  | 90.85   |                         |
|                    | MCI   | 86.18  | 88.60  | 80.86   | 0.834  | 88.1    |                         |

When the overall performance of both experiments is analyzed, it is observed that the models using gradient filter images increase the performance. Table 4 shows the overall performance values. When the table is analyzed, it is observed that the Densenet201 model shows the best results with 98.63%. It is thought that the reason why the Densenet201 model gives better results than the other models is that it carries the activation values from the first layer to the next layers. When the achievements are analyzed in Table 4, the models with the best performance are Vgg16, Resnet101, Resnet50, Vgg19 and Mobilenetv2 after Densenet201.

**Table 4.** Overall performance table for deep learning models using original and gradient filtered images

| Model Name         | Model Performances for Original Images | Model Performances for Gradient Preprocessed Images |
|--------------------|--|---|
| <b>DenseNet201</b> | 97.94                                  | 98.63   |
| <b>Resnet101</b>   | 94.05                                  | 95.42   |
| <b>Vgg16</b>       | 91.99                                  | 95.88   |
| <b>Resnet50</b>    | 89.24                                  | 93.14   |
| <b>Vgg19</b>       | 91.99                                  | 80.09   |
| <b>MobileNetv2</b> | 86.96                                  | 85.13   |

## 5 Conclusion

It has been observed that deep learning approaches, which are increasingly used in every field, also show good results in disease detection in the medical field. In this study, MR images are used for early detection of Alzheimer's disease. These MRI images consist of images taken from different axes and have different constraints. These differences may degrade the performance of the proposed approaches or result in misclassification. For this purpose, our proposed approaches aim to apply a preprocessing method to CNN models to eliminate such problems. In this way, it is envisaged to improve MRI images with different constraints taken from different axes. For this purpose, the original images were preprocessed using a gradient filter and the performance of the deep learning models was improved. As a result of the study, the Densenet201 model showed the best results of 97.94% and 98.63% for both original and preprocessed images, respectively. It is observed that gradient-based preprocessing improves the overall performance of deep learning models.

In future work, other filter methods used in preprocessing and deep learning methods will be designed. We will also investigate the detection of other stages of Alzheimer's disease.



### Conflict of interest

The authors declare no conflicts of interest.

**Similarity rate (iThenticate):** 18%

### Data availability statement

The main data supporting the findings of this study are openly available and can be obtained from the following address:

<https://www.kaggle.com/datasets/phamnguyenduytien/alzheimermri>.

### References

- [1] Z. Wang, et al., Classification of Alzheimer's disease, mild cognitive impairment and normal control subjects using resting-state fMRI based network connectivity analysis. *IEEE journal of translational engineering in health and medicine*, 6, 1-9, 2018. <https://doi.org/10.1109/JTEHM.2018.2874887>
- [2] S. Devkota, T.D. Williams, M.S.J.J. Wolfe, Familial Alzheimer's disease mutations in amyloid protein precursor alter proteolysis by  $\gamma$ -secretase to increase amyloid  $\beta$ -peptides of  $\geq 45$  residues. *Journal of Biological Chemistry*, 296, 2021. <https://doi.org/10.1016/j.jbc.2021.100281>
- [3] F. Feng, et al., Radiomic features of hippocampal subregions in Alzheimer's disease and amnesic mild cognitive impairment. *Frontiers in aging neuroscience*, 10, 290, 2018. <https://doi.org/10.3389/fnagi.2018.00290>
- [4] Chen, X., Li, L., Sharma, A., Dhiman, G., & Vimal, S., The application of convolutional neural network model in diagnosis and nursing of MR imaging in Alzheimer's disease. *Interdisciplinary Sciences: Computational Life Sciences*, 14 (1), 34-44, 2022. <https://doi.org/https://10.1007/s12539-021-00450-7>
- [5] Sarraf, S., & Tofighi, G., Classification of Alzheimer's disease using fMRI data and deep learning convolutional neural networks. *arXiv preprint arXiv:1603.08631*, 2016. <https://doi.org/10.48550/arXiv.1603.08631>
- [6] Q. Zhou, et al., An optimal decisional space for the classification of Alzheimer's disease and mild cognitive impairment. *IEEE Transactions on Biomedical Engineering*, 61 (8), 2245-2253, 2014. <https://doi.org/10.1109/TBME.2014.2310709>
- [7] G. Chen, et al., Classification of Alzheimer disease, mild cognitive impairment, and normal cognitive status with large-scale network analysis based on resting-state functional MR imaging. *Radiology*, 259 (1), 213, 2011. <https://doi.org/10.1148/radiol.10100734>
- [8] N. Yamanakkanavar, J.Y. Choi, B.J.S. Lee, MRI segmentation and classification of human brain using deep learning for diagnosis of Alzheimer's disease: a survey. *Sensors*, 20 (11), 3243, 2020. <https://doi.org/10.3390/s20113243>
- [9] R. Smith-Bindman, et al., Use of diagnostic imaging studies and associated radiation exposure for patients enrolled in large integrated health care systems, 1996-2010. *Jama*, 307(22), 2400-2409, 2012. <https://doi.org/10.1001/jama.2012.5960>
- [10] F. Ramzan, et al., A deep learning approach for automated diagnosis and multi-class classification of Alzheimer's disease stages using resting-state fMRI and residual neural networks. *Journal of medical systems*, 44 (2), 1-16, 2020. <https://doi.org/10.1007/s10916-019-1475-2>
- [11] H.A. Helaly, M. Badawy, A.Y. Haikal, Deep learning approach for early detection of Alzheimer's disease. *Cognitive Computation*, 14 (5), 1711-1727, 2022. <https://doi.org/10.1007/s12559-021-09946-2>
- [12] Mehmood, A., Maqsood, M., Bashir, M., & Shuyuan, Y., A deep Siamese convolution neural network for multi-class classification of Alzheimer disease. *Brain sciences*, 10 (2), 84, 2020. <https://doi.org/10.3390/brainsci10020084>
- [13] M. Mujahid, et al., An efficient ensemble approach for Alzheimer's disease detection using an adaptive synthetic technique and deep learning. *Diagnostics*, 13 (15), 2489, 2023. <https://doi.org/10.3390/diagnostics13152489>
- [14] A. Farooq, et al. A deep CNN based multi-class classification of Alzheimer's disease using MRI. *Proceedings of the 2017 IEEE International Conference on Imaging Systems and Techniques (IST)*, IEEE, 1-6, 2017. <https://doi.org/10.1109/IST.2017.8261460>
- [15] R. Ibrahim, R. Ghnemat, Q. Abu Al-Haija, Improving Alzheimer's disease and brain tumor detection using deep learning with particle swarm optimization. *AI*, 4(3), 551-573, 2023. <https://doi.org/10.3390/ai4030030>
- [16] P. Balaji, et al., Hybridized deep learning approach for detecting Alzheimer's disease. *Biomedicines*, 11(1), 149, 2023. <https://doi.org/10.3390/biomedicines11010149>
- [17] S. Basaia, et al., Automated classification of Alzheimer's disease and mild cognitive impairment using a single MRI and deep neural networks. *NeuroImage: Clinical*, 21, 101645, 2019. <https://doi.org/10.1016/j.nicl.2018.101645>
- [18] S. Liu, et al. Early diagnosis of Alzheimer's disease with deep learning. *Proceedings of the 2014 IEEE 11th International Symposium on Biomedical Imaging (ISBI)*, IEEE, 2014. <https://doi.org/10.1109/ISBI.2014.6868045>
- [19] Kaggle. Alzheimer-MRI|Kaggle. Available from: <https://www.kaggle.com/datasets/phamnguyenduytien/alzheimermri>, July 10, 2022.
- [20] C.C. Aggarwal, *Neural networks and deep learning*. Springer, 10(978), 3, 2018.
- [21] S. Sharma, S. Sharma, A. Athaiya, Activation functions in neural networks. *Towards Data Science*, 6 (12), 310-316, 2017. <https://doi.org/10.33564/IJEAST.2020.v04i12.054>
- [22] L. Zhou, et al., Machine learning on big data: Opportunities and challenges. *Neurocomputing*, 237,

- 350-361, 2017. <https://doi.org/10.1016/j.neucom.2017.01.026>
- [23] S.H. Lee, et al., How deep learning extracts and learns leaf features for plant classification. *Pattern Recognition*, 71, 1-13, 2017. <https://doi.org/10.1016/j.patcog.2017.05.015>
- [24] M.D. Zeiler, G.W. Taylor, R. Fergus. Adaptive deconvolutional networks for mid and high level feature learning. *Proceedings of the 2011 International Conference on Computer Vision*, IEEE, 2011. <https://doi.org/10.1109/ICCV.2011.6126474>
- [25] A. Apicella, et al., A survey on modern trainable activation functions. *Neural Networks*, 138, 14-32, 2021. <https://doi.org/10.1016/j.neunet.2021.01.026>
- [26] P. Wang, E. Fan, P. Wang, Comparative analysis of image classification algorithms based on traditional machine learning and deep learning. *Pattern Recognition Letters*, 141, 61-67, 2021. <https://doi.org/10.1016/j.patrec.2020.07.042>
- [27] S. Jia, et al., A survey: Deep learning for hyperspectral image classification with few labeled samples. *Neurocomputing*, 448, 179-204, 2021. <https://doi.org/10.1016/j.neucom.2021.03.035>
- [28] U. Ruby, V. Yendapalli, Binary cross entropy with deep learning technique for image classification. *International Journal of Advanced Trends in Computer Science and Engineering*, 9 (10), 2020. <https://doi.org/10.30534/ijatcse/2020/175942020>
- [29] D. Theckedath, R. Sedamkar, Detecting affect states using VGG16, ResNet50 and SE-ResNet50 networks. *SN Computer Science*, 1, 1-7, 2020. <https://doi.org/10.1007/s42979-020-0114-9>
- [30] A. Karacı, VGGCOV19-NET: automatic detection of COVID-19 cases from X-ray images using modified VGG19 CNN architecture and YOLO algorithm. *Neural Computing and Applications*, 34(10), 8253-8274, 2022. <https://doi.org/10.1007/s00521-022-06918-x>
- [31] M. Yildirim, A. Çınar, E. Cengil, Classification of the weather images with the proposed hybrid model using deep learning, SVM classifier, and mRMR feature selection methods. *Geocarto International*, 37 (9), 2735-2745, 2022. <https://doi.org/10.1080/10106049.2022.034989>
- [32] A. Jaiswal, et al., Classification of the COVID-19 infected patients using DenseNet201 based deep transfer learning. *Journal of Biomolecular Structure and Dynamics*, 39 (15), 5682-5689, 2021. <https://doi.org/10.1080/07391102.2020.1788642>
- [33] J.C. Koh, G. Spangenberg, S. Kant, Automated machine learning for high-throughput image-based plant phenotyping. *Remote Sensing*, 13(5), 858, 2021. <https://doi.org/10.3390/rs13050858>
- [34] A.G. Howard, et al., Mobilenets: Efficient convolutional neural networks for mobile vision applications. *arXiv preprint arXiv:1704.04861*, 2017.
- [35] H. Lu, et al., FDCNet: filtering deep convolutional network for marine organism classification. *Multimedia Tools and Applications*, 77, 21847-21860, 2018. <https://doi.org/10.1007/s11042-017-4585-1>
- [36] A. Shabbir, et al., Satellite and scene image classification based on transfer learning and fine tuning of ResNet50. *Mathematical Problems in Engineering*, 2021, 1-18, 2021. <https://doi.org/10.1155/2021/5843816>
- [37] M. Toğaçar, Detection of retinopathy disease using morphological gradient and segmentation approaches in fundus images. *Computer Methods and Programs in Biomedicine*, 214, 106579, 2022. <https://doi.org/10.1016/j.cmpb.2021.106579>
- [38] J. Na'am, et al., Filter technique of medical image on multiple morphological gradient (MMG) method. *TELKOMNIKA (Telecommunication Computing Electronics and Control)*, 17 (3), 1317-1323, 2019. <https://doi.org/10.12928/telkomnika.v17i3.9722>
- [39] M. Nakashizuka, Image regularization with multiple morphological gradient priors. *Proceedings of the 2016 IEEE International Conference on Image Processing (ICIP)*, IEEE, 2016. <https://doi.org/10.1109/ICIP.2016.7532973>
- [40] M. TOĞAÇAR, B. ERGEN, M.E. SERTKAYA, Zatürre hastalığının derin öğrenme modeli ile tespiti. *Firat University Journal of Engineering*, 31 (1), 223-230, 2019.

